Electronic Supplementary Material (ESI) for Sustainable Energy & Fuels.

Supporting Information

Atomic layer deposition of vanadium oxide to reduce parasitic absorption and improve stability in n-i-p perovskite solar cells for tandems

James A. Raiford[1†], Rebecca A. Belisle[2,3†], Kevin A. Bush[3], Rohit Prasanna[3,4], Axel F. Palmstrom[4], Michael D. McGehee[5], Stacey F. Bent*[1]

[1] Department of Chemical Engineering, Stanford University, Stanford, CA 94305, USA
[2] Physics Department, Wellesley College, Wellesley, MA 02481, USA
[3] Department of Materials Science and Engineering, Stanford University, Stanford, CA 94305, USA
[4] National Renewable Energy Laboratory, Golden, Colorado 80401, USA
[5] Department of Chemical and Biological Engineering, University of Colorado, Boulder, CO 80309, USA

[†]These authors contributed equally to this work.
*Corresponding author: sbent@stanford.edu

Experimental Methods

Anti-solvent Perovskite Deposition

To make the 1.0M $Cs_{0.17}FA_{0.83}Pb(Br_{0.17}I_{0.83})_3$ perovskite precursor solution, stoichiometric amounts of lead iodide (TCI), lead bromide (TCI), cesium iodide (Sigma-Aldrich) and formamidinium iodide (Dyesol) were combined in a 1:1 mixture of N,N-dimethylformamide (Sigma-Aldrich) and dimethyl sulfoxide (Sigma-Aldrich). We made the solution at least six hours prior to perovskite film fabrication and mixed it on a stir plate to help dissolve the precursor salts. Spin-coating of the films was done in a dry-air glove box with < 1 ppm H_2O. Two drops of the precursor solution were deposited on a substrate through a 0.2 μm PTFE filter and spread over the entire substrate using a pipette tip. The spin-coating recipe consisted of two steps: 10 seconds at 1000 rpm with an acceleration of 500 rpm/s and 35 seconds at 6000 rpm with a 3000 rpm/s acceleration. During the last five seconds of the second step, 90 μL of chlorobenzene (Sigma-Aldrich) was pipetted onto the center of the substrate to act as an anti-solvent and nucleate perovskite crystallization. After spinning, the substrate was transferred to a hot plate at 60 °C for approximate 5 seconds until the entire film converted to a dark grey. The substrate was then transferred to a hot plate at 100 °C and annealed for 30-60 minutes.

Device Fabrication

2 cm x 2 cm patterned indium tin oxide (ITO) substrates (Xin Yan Technology) with a sheet resistance of 10 Ω/□ were used for both opaque and semi-transparent devices. The substrates were first sonicated in Extran alkaline solution, acetone and isopropanol, each for 10 minutes, followed by 15 minutes of UV-ozone cleaning.

To make the tin oxide nanoparticle layer, 15 wt% tin oxide in water colloidal suspension (Alfa-Aesar) was sonicated for 30 minutes, before diluting it 1:3 by volume with deionized water. Two drops of the diluted suspension were then dispersed onto the ITO substrate through a 0.45μL hydrophilic PTFE filter and spun on the substrate at 4000 rpm for 30 seconds. Immediately after spinning, the substrates were annealed in air at 150 °C for 1 hour. The 15 nm C_{60} layer was deposited by thermal evaporation at a rate of 0.15 Å/s in an Angstrom Amod evaporator while cooling the substrates to 0 °C during the evaporation.

The perovskite layer was spin-coated using the procedure described in the previous section. For some devices doped spiro-OMeTAD was used as a hole transport layer. The spiro-OMeTAD solution was made by dissolving 72.3 mg of spiro-OMeTAD (Lumtec) in chlorobenzene (Sigma-Aldrich) and then adding 17.5 μL of 520 mg/mL LiTFSI dopant (Sigma-Aldrich) in acetonitrile (Sigma-Aldrich) before stirring for 15 minutes on a 70 °C hotplate. After allowing the solution to cool, 28.8 μL of tert-butylpyridine (Sigma Aldrich) was added and the solution was filtered through a 0.2 μm PTFE filter. For each device, 60 μL of spiro-OMeTAD solution was spun at 4000 rpm for 30 seconds with a 2000 rpm/s acceleration.

The 30 nm spiro-TTB (Lumtec) hole transport layer was deposited via thermal evaporation in the same Angstrom evaporator using a baffle box and a deposition rate of 0.1 Å/s for the first 10 nm and 1 Å/s for the remaining 20 nm. The substrates were cooled to 0 °C throughout the evaporation. Next, the vanadium oxide sputter buffer layer was deposited using the procedure described in the subsequent section.

For opaque devices, 100 nm of gold was thermally evaporated through a shadow mask to create the top electrode and to make good electrical contact with exposed bottom ITO on the edges of the device; the evaporation rate was 0.2 Å/s for the first 10 nm and 2 Å/s for the remaining 90 nm. For semi-transparent devices, a 150 nm layer of ITO was deposited via DC magnetron sputtering for the top electrode with a base pressure of 5×10^{-6} torr, a deposition pressure of 2×10^{-3} torr and 5% oxygen partial pressure. The semi-transparent devices were finished with 130 nm silver fingers thermally evaporated through a shadow mask with the same deposition rates as the gold electrodes.

Vanadium Oxide ALD/pulsed-CVD

The vanadium oxide sputter buffer layer was developed using an Arradiance Gemstar-6 ALD system. Vanadium(V) oxytriisopropoxide (VTIP) (Strem Chemicals) was used as the metal-organic precursor and deionized water as the counter-reactant. The vanadium precursor and water bubblers were held at 50 °C and room temperature, respectively, and the reactor manifolds were set to 115 °C. The reactor temperature was set to 80°C. Each cycle consisted of the following sequence: 2 second VTIP pulse (30 sccm N_2), 3 second VTIP purge (90 sccm N_2), 2 second H_2O pulse (30 sccm N_2), 3 second H_2O purge (90 sccm N_2). In addition, a short pump block was introduced for both the VTIP and H_2O half cycles to increase the residence time of the precursors in the reaction chamber. Each pump block sequence consisted of: closing the valve to the pump line prior to pulsing the precursor/counter-reactant, holding the pump valve closed for 3 seconds (15 sccm N_2) following the pulse, then opening the pump value to allow for the purging of excess precursor and by-products. As shown in Figure S1, this longer exposure time was necessary to achieve saturating growth behavior and has been observed previously for this ALD chemistry.[1] The resulting growth rate of the VO_x film at 80°C was approximately 0.40 Å/cycle.

X-Ray Diffraction

The X-ray diffraction spectra were collected using a PANalytical X'Pert PRO system. The diffractometer uses an incident beam of Cu Kα radiation (1.542 Å). For each scan, a 1/2° divergence slit and 15 mm mask were employed to control the equatorial and axial width of the incident beam, respectively, and a 0.27° parallel plate collimator was used to define the acceptance angle of the diffracted beam. The XRD spectra of the perovskite films were collected using symmetric 2θ-ω scans. A fixed incident angle of $\omega = 4°$ was used for the grazing incidence XRD spectra of the ALD VO_x and Si (100) substrate.

X-Ray Photoelectron Spectroscopy

X-ray photoelectron spectroscopy measurements were performed with a PHI Versaprobe 3 system which uses monochromatized Al Kα (1486 eV) radiation. The scans were taken with a 200 μm beam size, 50 W beam power and 15 kV e-beam energy. For some samples, an argon gas cluster ion beam gun (GCIB) was used to remove adventitious carbon from the surface. The peak positions were normalized by aligning the O1s peak of vanadium oxide to 530.0 eV.

A Shirley background was used when fitting the V2p and O1s peaks. The peak shapes were assumed to be Gaussian-Lorentz, with the relative percentage of Gaussian behavior allowed to fluctuate between 50% and 100% for each curve to obtain the best fit. The splitting of the two

V^{5+} peaks and the two V^{4+} peaks were both fixed to 7.3 eV, based on a previous XPS study of VO_x thin films.[2] The areas under the V^{5+} and V^{4+} peaks in the $V2p_{3/2}$ state were fixed to be twice the areas under the corresponding V peaks in the $V2p_{3/2}$ state based on spin-orbit degeneracy rules.

Atomic Force Microscopy

The atomic force micrographs were taken with a Park NX-10 scanning probe microscope. The scans were taken in non-contact mode with a Park ACTA cantilever (300 kHz resonance frequency, <10 nm tip radius) and a 0.5 Hz scan rate.

Transmittance/Reflectance Measurements

Transmittance and reflectance measurements were taken with a Jasco Model V-670 UV-Vis-NIR spectrometer with a 60mm integrating sphere at a scan speed of 2000 nm/min.

Solar Cell J-V and EQE Measurements

A Keithley 2400 digital source meter was used for current-voltage measurements of the solar cells. Devices were illuminated through either the glass side or front ITO electrode with a Xe 300W (Oriel) solar simulator lamp. A silicon reference photodiode was used to calibrate the solar lamp to match measured EQE currents. The active areas for opaque and semi-transparent devices were defined by masks with aperture areas of 0.12 and 0.39 cm^2, respectively. Devices were scanned from forward to reverse bias over the range 1.2V to -0.2V. A perturb and measure LABVIEW based program was used to track the maximum-power-point of the devices.

EQE measurements of the perovskite cells were taken using a QEX7 solar cell spectral response system from PV Measurements. Light from a 65 W xenon arc lamp source was passed through a dual grating monochromator, filtered and then chopped at a frequency of 100 Hz before being split between a reference silicon cell and the test device. The responses of both devices were measured simultaneously to account for light fluctuations. The EQE of the test device was calculated by comparing the photocurrent of the test device to that of a calibrated silicon reference photodiode.

Spectroscopic Ellipsometry

For each ALD VO_x deposition, a small piece of a Si (100) polished wafer was UV-ozone cleaned for 10 minutes and then placed inside the ALD reactor. Film thicknesses of the ALD VO_x were estimated by fitting an optimized Cauchy film model to spectroscopic ellipsometry data taken on a J.A. Woollam Co., Inc. α-SE ellipsometer. Each measurement included two scans at incident light angles of 65° and 70° over a 380 nm to 900 nm wavelength range. Woollam CompleteEASE software was used to perform the fittings. ALD VO_x films of three different thicknesses were simultaneously fit to determine the Cauchy dispersion equation parameters for the model. The model also included a 13.5 Å native SiO_2 layer on top of the Si substrate.

Solar Cell Modeling

Simulations of the absorption, transmission and reflection spectra of the semi-transparent perovskite solar cells were performed using a transfer matrix optical model developed by G. F. Burkhard et al. More details regarding the model are included in their published

communication.[3] The script is also available at http://mcgehee.group.stanford.edu/transfermatrix. The approximate thickness and optical constants (n & k) of each layer in the device stack were used as inputs into the model. The model does not factor in roughness of the individual layers. The optical constants for all of the layers in the perovskite sub-cell apart from the HTMs and VO_x, as well as the ITO recombination layer and a-Si contact layers in the simulated 2-terminal PSC/c-Si tandem, were obtained from a previous study by S. Manzoor et al.; a detailed description of the optical constant measurements is included in the experimental section of that work.[4] For the modeling of the tandem device, c-Si with an infinite thickness was used to approximate the light absorber in the Si heterojunction sub-cell. The optical constants of the c-Si layer were obtained from spectral photoluminescence measurements published by H.T. Nguyen et al.[5] The optical constants of the spiro-OMeTAD layer were obtained from a perovskite optical simulation study by M. Filipič et al.[6]

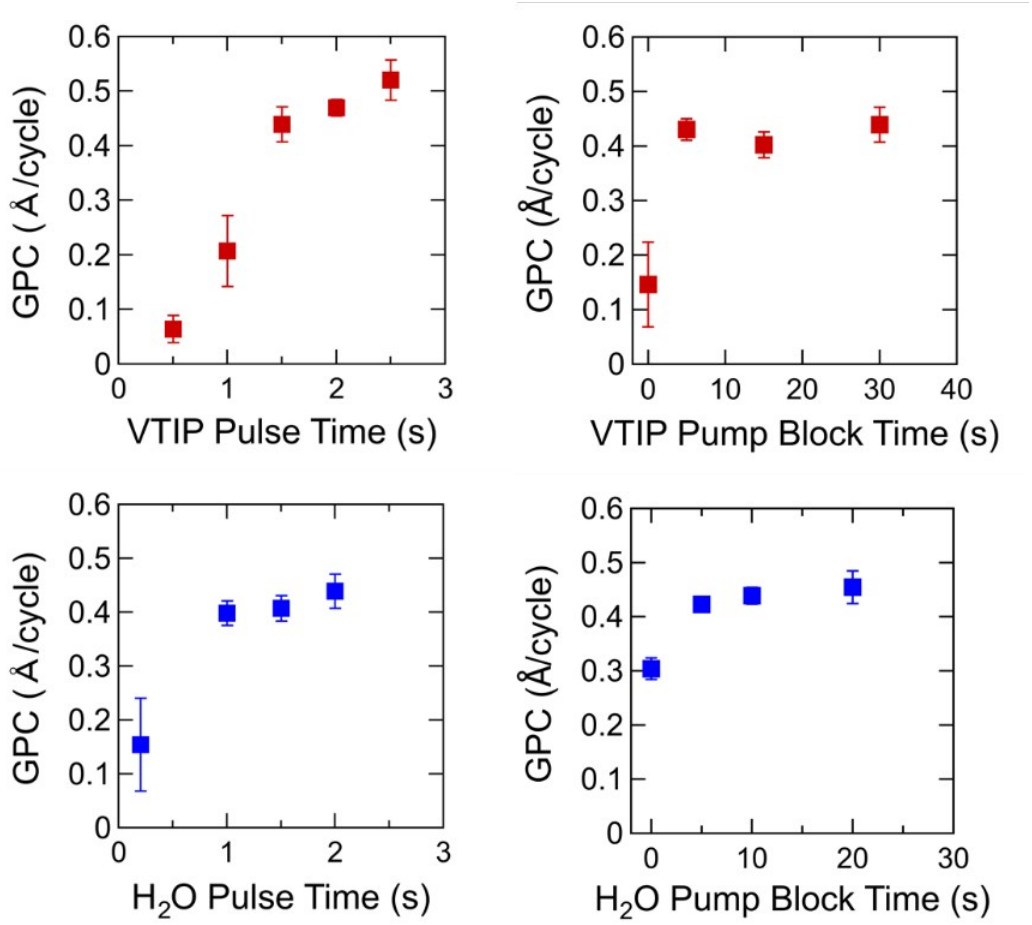

Figure S1: Growth curves for the ALD of vanadium oxide from vanadium oxytriisopropoxide (VTIP) and H_2O at a reactor temperature of 100 °C. Film growth per cycle (GPC) is plotted as a function of pulse time and pump block time for both VTIP and H_2O with half-cycle purge times of 30 seconds. VTIP and H_2O pulse times of 2 seconds each were used for the pump block time experiments. A 30 second H_2O pump block was used for the VTIP pump block time experiment. A 5 second VTIP pump block was used for the H_2O pump block time experiment.

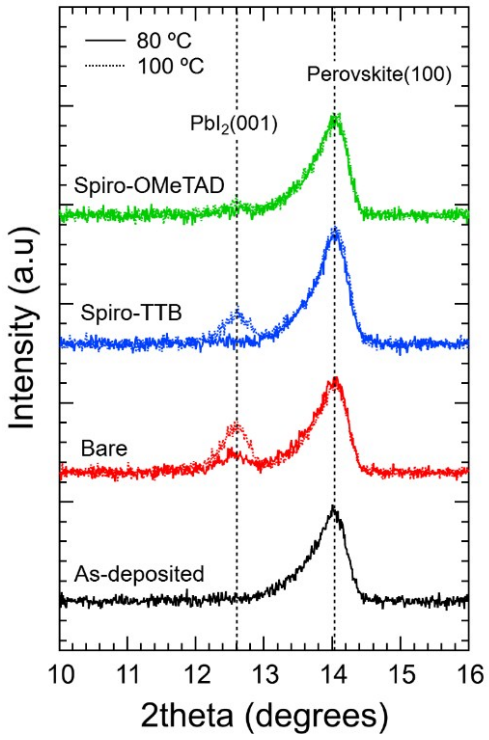

Figure S2: XRD data showing the PbI_2(001) and $Cs_{0.17}FA_{0.83}Pb(Br_{0.17}I_{0.83})_3$ perovskite (100) peaks for an as-deposited perovskite film and for perovskite films after ALD VO_x processing at 80°C and 100°C both with and without an interface organic HTL.

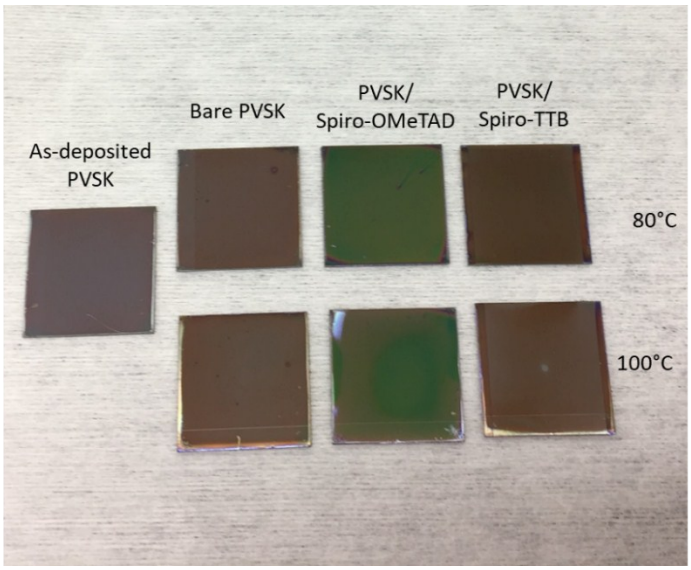

Figure S3: Images of an as-deposited $Cs_{0.17}FA_{0.83}Pb(Br_{0.17}I_{0.83})_3$ perovskite film and perovskite films after ALD VO_x processing at 80°C and 100°C both with and without an interface organic HTL.

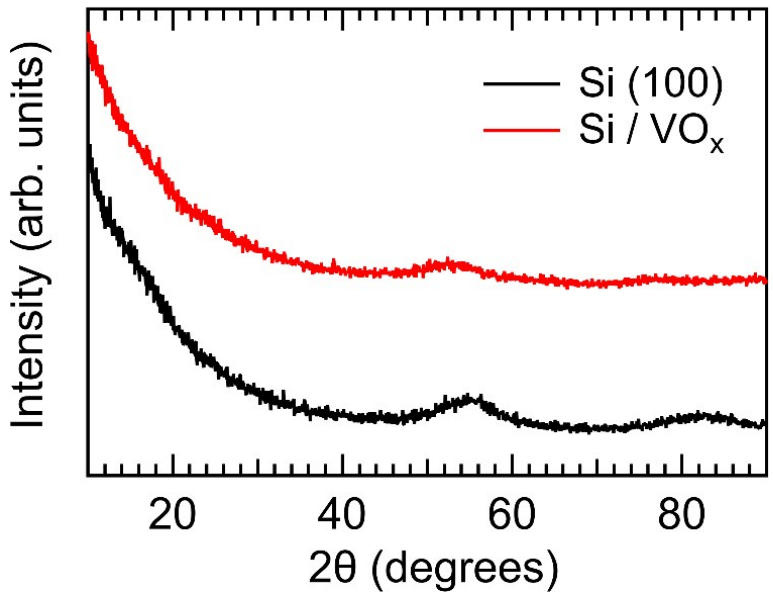

Figure S4: Grazing incidence XRD spectra of a bare Si (100) substrate (bottom) and a 9 nm thin film of ALD VO_x grown at 80°C on a Si (100) substrate (top). A fixed incident angle of 4° was used for both measurements.

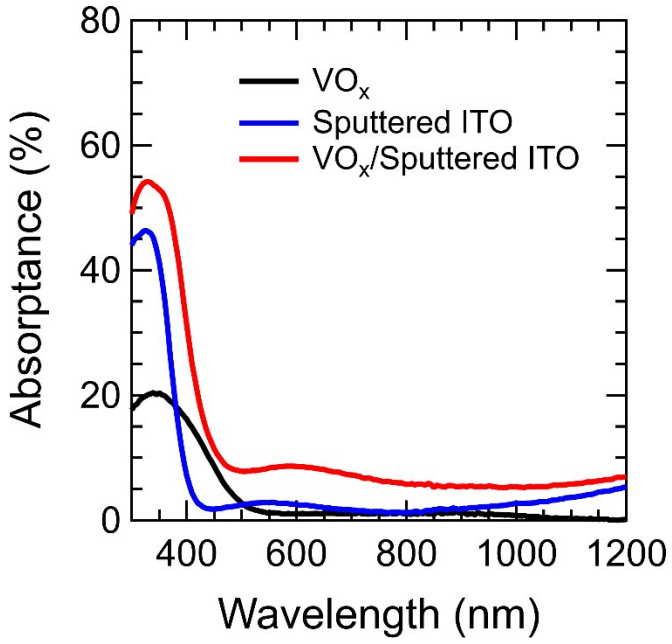

Figure S5: Absorption spectra of a 9 nm ALD VO_x film, a 150 nm sputtered ITO film, and a 150 nm of ITO sputtered on top of a 9 nm ALD VO_x film, all on quartz substrates.

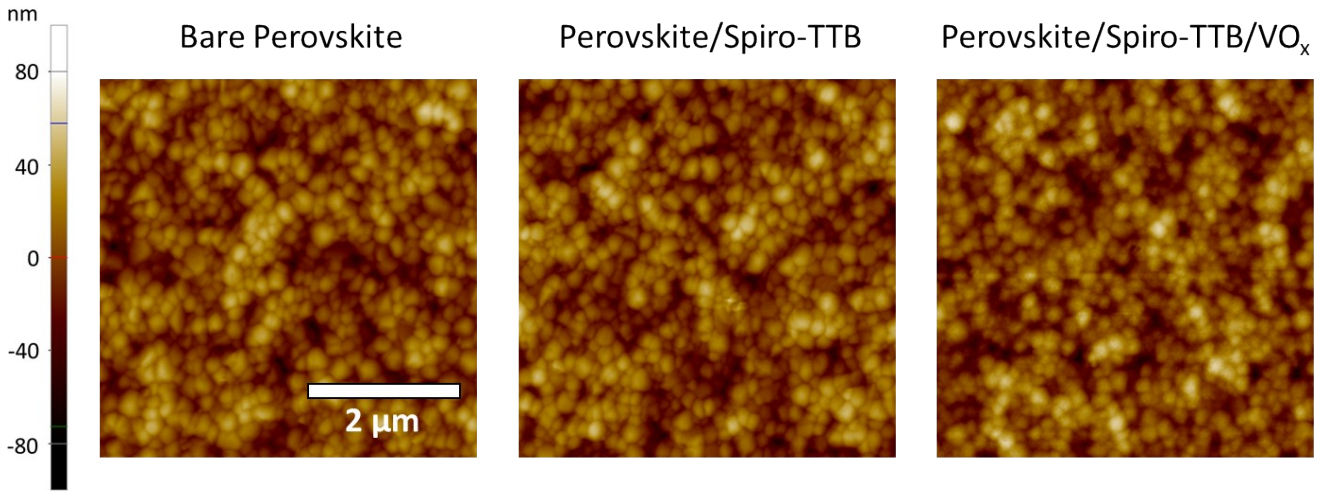

Figure S6: 5µm x 5µm atomic force microscopy (AFM) images of 17/17 perovskite films before and after the subsequent deposition of spiro-TTB and ALD VO_x HTLs.

Table S1: Surface topographic parameters (average roughness (R_a), root mean square roughness (R_q), skewness (R_{sk}) and kurtosis (R_{ku})) measured by AFM corresponding to the 3 images in Figure S6.

Film Stack	**R_a (nm)**	**R_q (nm)**	**R_{sk}**	**R_{ku}**
perovskite	14.3	17.8	0.058	2.86
perovskite/spiro-TTB	14.7	18.3	0.077	2.84
perovskite/spiro-TTB/VO_x	15.3	19.2	0.016	2.98

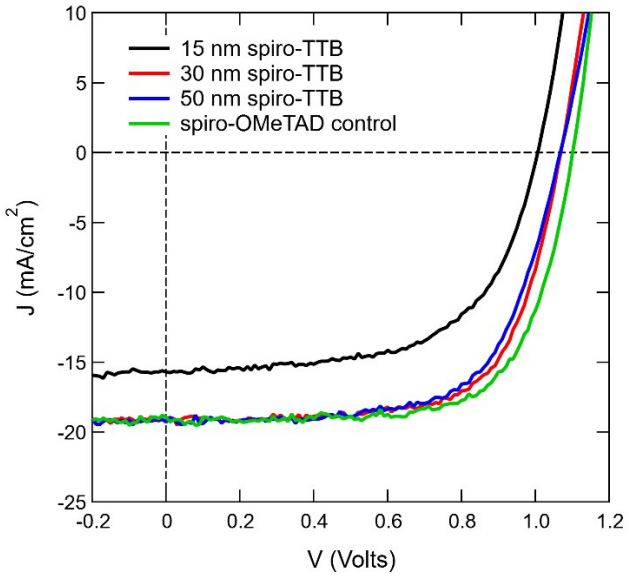

Figure S7: Current-voltage curves for opaque solar cell with VO_x with varying thickness of the spiro-TTB HTL.

$$R\left[\Omega \cdot cm^2\right] = \rho_{ttb} t_1 + R_{C,Ag/ttb} + R_{C,ttb,ITO} + R_{s,ITO} L_2 L_1 + R_{C,probe}$$

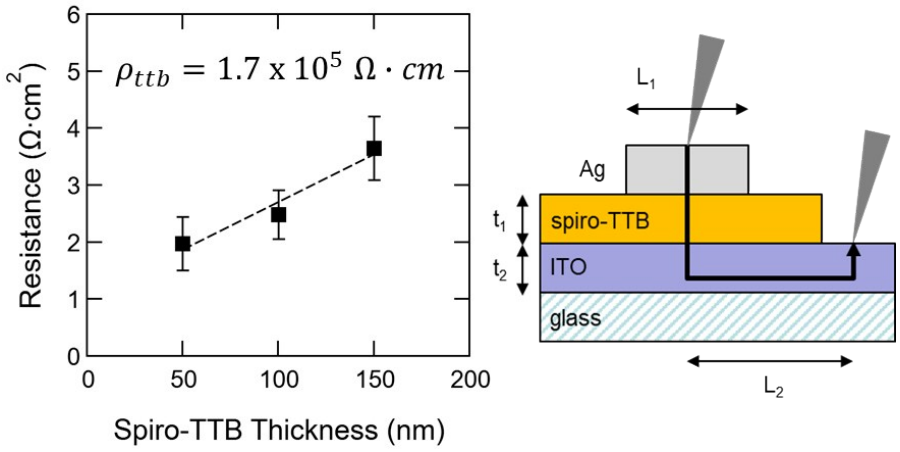

Figure S8: Resistivity of the evaporated spiro-TTB layer extracted from resistance data for various spiro-TTB thicknesses (left). A cross-sectional schematic of the device structure used for the resistance measurements (right) and the corresponding equation used to calculate spiro-TTB resistivity (ρ_{ttb}) (top). 'R' is the total resistance measured between the two probes, 't_1' is the thickness of the spiro-TTB, '$R_{C,Ag/ttb}$' is the contact resistance between the silver (Ag) and spiro-TTB, '$R_{C,ttb/ITO}$' is the contact resistance between the ITO and spiro-TTB, '$R_{s,ITO}L_1L_2$' is the in-plane resistance through the ITO, and '$R_{C,probe}$' is contact resistance from the probes. The sum of these last four resistance terms corresponds to the y-intercept of the R vs. t_1 plot.

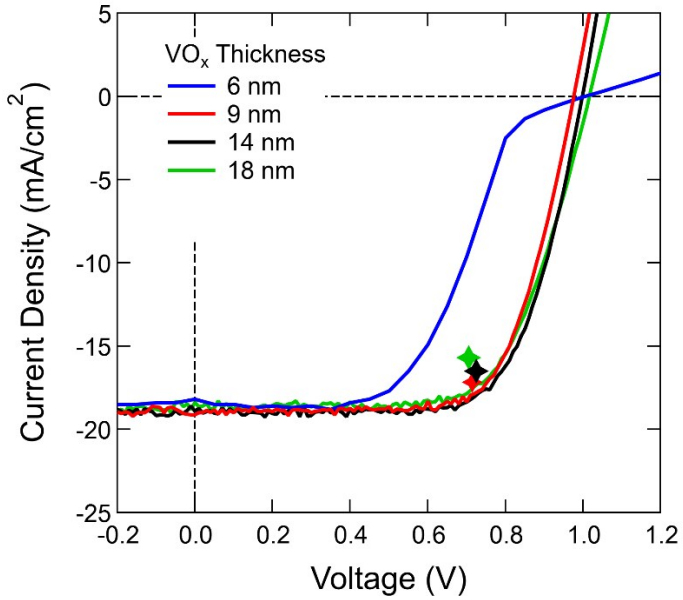

Figure S9: Current-voltage curves for semi-transparent solar cells with a spiro-OMeTAD HTL and varying thickness of the VO_x sputter buffer layer. The stars represent the steady-state maximum power points for the devices after 1000 seconds of continuous illumination.

Table S2: Performance parameters corresponding to the J-V curves and maximum power point tracking (MPPT) of the opaque and semi-transparent device from Figure 2c.

		J-V Curves				**MPPT**	
	HTL	**J_{SC} (mA/cm2)**	**V_{OC} (V)**	**FF (%)**	**η (%)**	**Initial η (%)**	**Stabilized η (%)**
Opaque	spiro-TTB	18.9	1.07	71	14.2	14.2	13.9
	spiro-OMeTAD	18.3	1.05	73	14.1	14.1	13.6
Semi-transparent	spiro-TTB	17.1	1.06	73	13.2	13.2	12.3
	spiro-OMeTAD	17.2	1.02	75	13.4	13.1	12.9

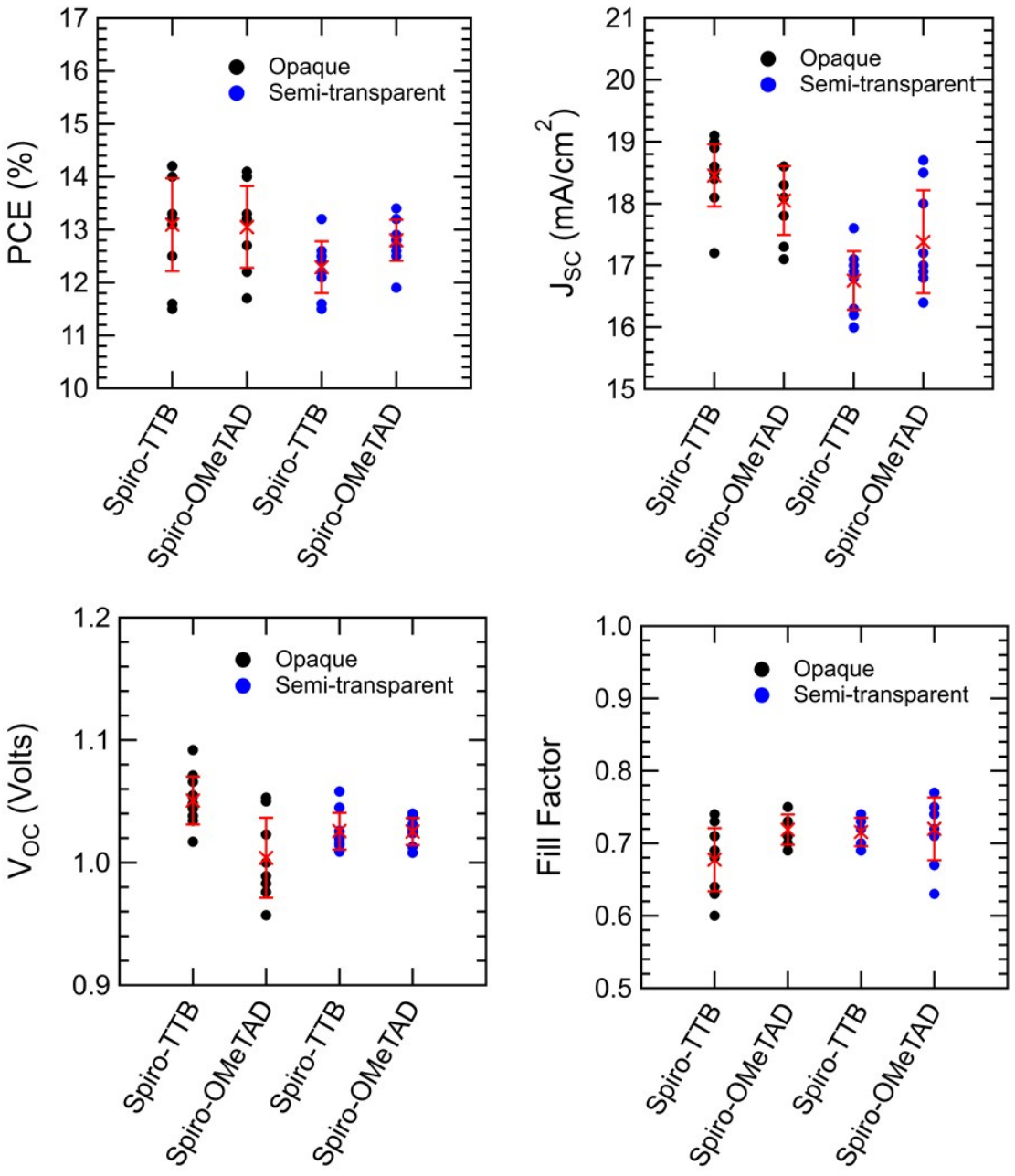

Figure S10: Performance parameters of both opaque (black circles) and semi-transparent (blue circles) PSCs with both spiro-TTB (11 opaque and 9 semi-transparent devices) and spiro-OMeTAD (8 opaque and 11 semi-transparent devices) HTLs. Averages of each subset are indicated by a red cross and +/- one-standard deviations are shown by the red lines.

Table S3: Summary of performance statistics for the opaque and semi-transparent PSCs from Figure S10. Both the average and standard deviation are provided for each parameter.

	HTL	J_{SC} (mA/cm2)	V_{OC} (V)	FF	η (%)
Opaque	spiro-TTB	18.5 ± 0.50	1.05 ± 0.02	0.68 ± 0.04	13.1 ± 0.88
	spiro-OMeTAD	18.1 ± 0.56	1.00 ± 0.03	0.72 ± 0.02	13.1 ± 0.77
Semi-transparent	spiro-TTB	16.8 ± 0.47	1.03 ± 0.01	0.72 ± 0.02	12.3 ± 0.49
	spiro-OMeTAD	17.4 ± 0.83	1.03 ± 0.01	0.72 ± 0.04	12.8 ± 0.39

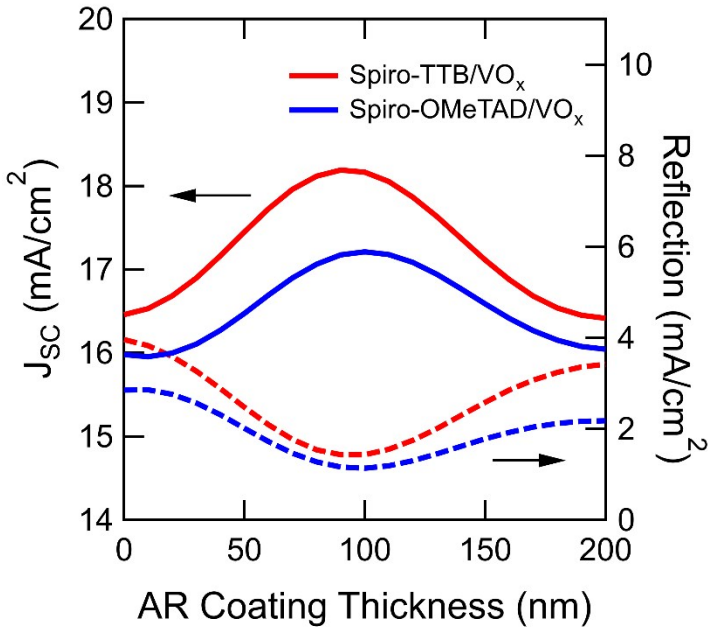

Figure S11: MgF_2 anti-reflective coating thickness optimization results obtained using transfer matrix modeling of the semi-transparent cells whose performances are shown in Figure 3. In the optimal case, short-circuit current in the perovskite cell (solid lines) should be maximized and total reflection between wavelengths of 300-760 nm (dashed lines) should be minimized.

Table S4: Performance parameters corresponding to the J-V curves for the semi-transparent devices illuminated through the front ITO contact in Figure 3b.

HTL	J_{SC} (mA/cm^2)	V_{OC} (V)	FF (%)	η (%)
spiro-TTB	18.9	1.06	67	13.4
spiro-OMeTAD	16.6	1.03	78	13.3

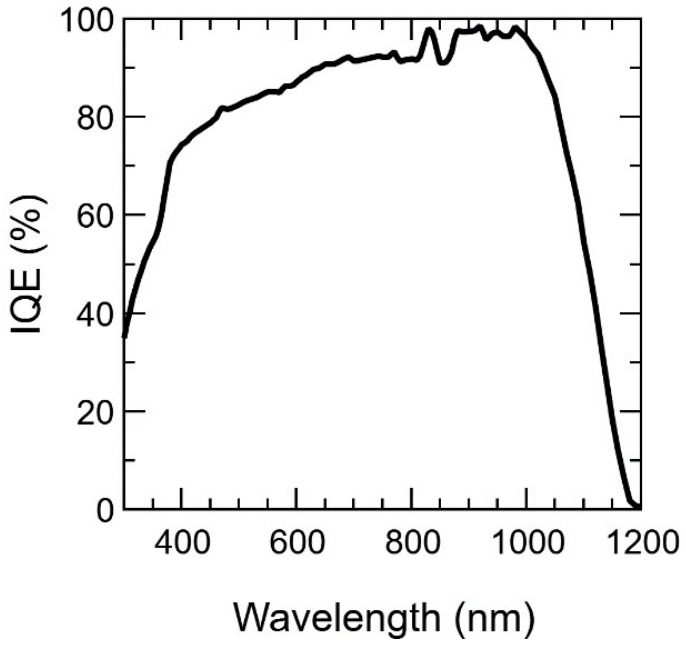

Figure S12: Internal quantum efficiency (IQE) of a representative silicon HIT cell used for modeling the photocurrent in the low bandgap sub-cell of n-i-p tandems.

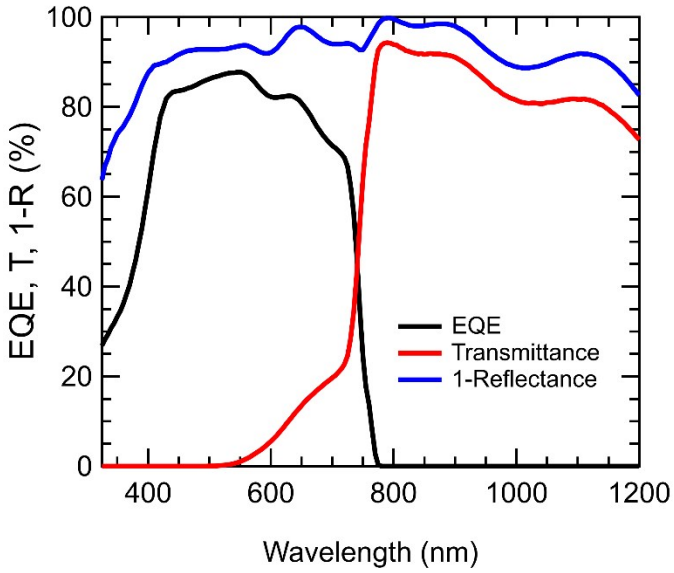

Figure S13: Predicted EQE, transmission, and reflection spectra for the front perovskite sub-cell of an n-i-p, two-terminal perovskite/c-Si tandem with the spiro-TTB/VO_x bilayer. The spectra were obtained using one-dimensional transfer matrix modeling described in the experimental methods section. The simulated device stack includes: MgF_2 (100nm)/ITO (40nm)/VO_x (9nm)/spiro-TTB (30nm)/17/17 perovskite (415nm)/C_{60} (15nm)/SnO_2 (40nm)/ITO (160nm)/a-Si:H(p) (15 nm)/a-Si:H(i) (7nm)/c-Si (infinite thickness). The inputs to the model were the thicknesses and optical constants (n & k) of each layer.

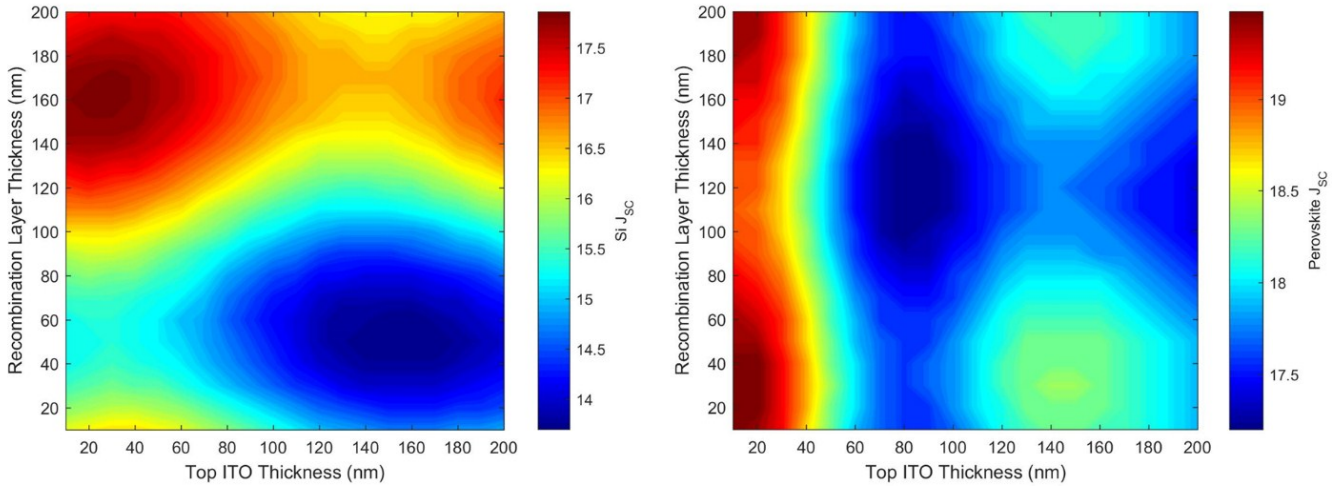

Figure S14: Two-dimensional maps generated using one-dimensional transfer matrix modeling that show the photocurrents generated in perovskite (right) and silicon (left) sub-cells of a n-i-p 2-terminal tandem for various thicknesses of the ITO recombination layer and top contact. The simulated tandem stack is identical to the one from Figure S13.

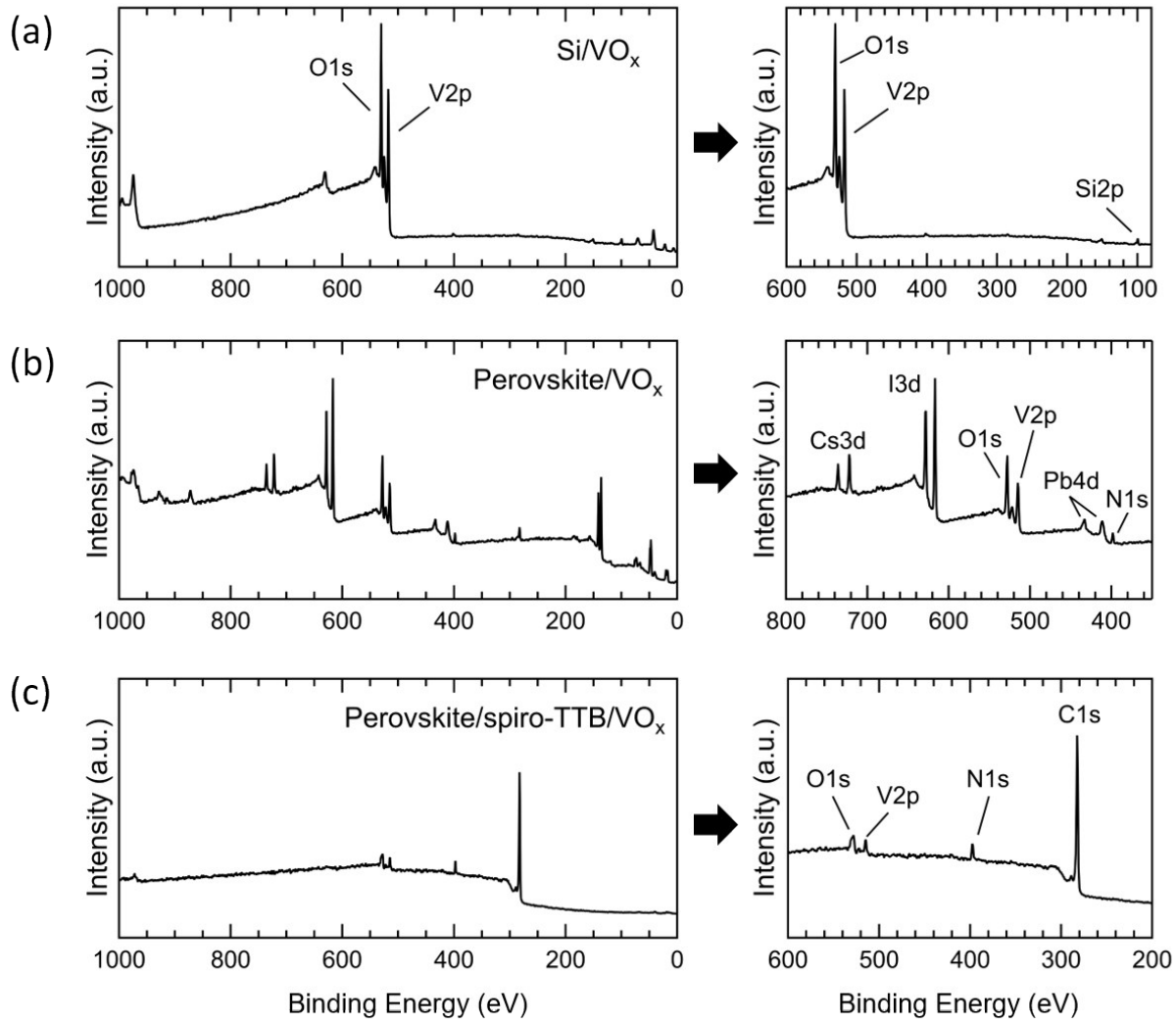

Figure S15: XPS survey spectra corresponding to the high resolution V2p, O1s spectra in Figure 4a. In each case, 100 cycles of ALD VO_x (~4 nm) were deposited on top of (a) polished silicon (b) a 17/17 perovskite film and (c) 30 nm of spiro-TTB on a 17/17 perovskite film. In each panel, the peaks relevant to the substrate are zoomed in on and labeled in the plot to the right.

References

1 J. Musschoot, D. Deduytsche, H. Poelman, J. Haemers, R. L. Van Meirhaeghe, S. Van den Berghe and C. Detavernier, *J. Electrochem. Soc.*, 2009, **156**, 122–126.

2 G. Silversmit, D. Depla, H. Poelman, G. B. Marin and R. De Gryse, *J. Electron Spectros. Relat. Phenomena*, 2004, **135**, 167–175.

3 G. F. Burkhard, E. T. Hoke and M. D. McGehee, *Adv. Mater.*, 2010, **22**, 3293–3297.

4 S. Manzoor, J. Hausele, K. A. Bush, A. F. Palmstrom, J. Carpenter, Z. J. Yu, S. F. Bent, M. D. McGehee and Z. C. Holman, *Opt. Express*, 2018, **26**, 27441.

5 H. T. Nguyen, F. E. Rougieux, B. Mitchell and D. Macdonald, *J. Appl. Phys.*, 2014, **115**, 043710.

6 M. Filipič, P Löper, B. Niesen, S. De Wolf, J. Krč, C. Ballif and M. Topič, *Opt. Express*, 2015, **23**, A263-A278.